Journal of Engineering Mathematics, Vol. 8, No. 1, January 1974
Noordhoff International Publishing–Leyden
Printed in The Netherlands

A study of cracks in orthotropic crystals using dislocation layers

G. E. TUPHOLME*

Department of Mathematics, Simon Fraser University, Burnaby, B. C., Canada

(Received May 28, 1973)

SUMMARY

The method of dislocation layers is used to study the stress field of a loaded Griffith-type elastic strip crack in an orthotropic crystal. Three fundamental modes of tractions applied to the crack faces are discussed. Formal solutions are derived for the stress components and the distribution of stress near a crack tip is deduced, before representative numerical results are presented graphically. Finally, the method is applied to the BCS model of elastoplastic cracks. In particular, the results are convenient for studying certain orientations of elastic and elastoplastic cracks in hexagonal and cubic crystals.

1. Introduction

The stress fields created in isotropic, homogeneous, elastic and elastoplastic media by applying loads to the surfaces of cracks of Griffith type have been studied quite extensively (see [1], [2] and further references given in these books). A large portion of the literature has been concerned with finding either exact or approximate solutions to these problems using integral transform techniques and the methods of complex potential function theory. The application of corresponding techniques to crack problems in anisotropic materials is rather cumbersome.

However, in 1948 Zener [3] and later Friedel [4] pointed out that many straight cracks can be represented by continuous distributions of dislocations. Several authors have subsequently used this powerful technique and substantial summaries of their work are included in the accounts by Bilby and Eshelby [5] and Lardner [6]. Recently, Lardner [7] and Guidera [8] have demonstrated that the method is also applicable for solving a large class of boundary value problems of classical elasticity, and Tupholme and Lardner [9] have used similar techniques for discussing moving cracks. The stress field of dislocations in homogeneous anisotropically elastic solids for a three dimensional state of stress in which the stress is independent of one Cartesian coordinate has been developed by Eshelby [10] and Eshelby, Read and Shockley [11], and later more fully in a general context by Stroh [12].

The purpose of the present paper is to show that the dislocation layer method can be applied in a straightforward manner to an investigation of the stress field of particular orientations of a loaded straight crack in an orthotropic crystal. Recently, Chou and Sha [13] have stated the components of the stress fields for a glide edge dislocation, a climb edge dislocation and a screw dislocation in such a material. Their results generalize those given previously by Chou [14] for dislocations in a basal plane of a hexagonal crystal and by Chou, Garofalo and Whitmore [15] and Chou and Whitmore [16] for a cubic crystal. These expressions provide the starting point of the present analysis.

Whilst this investigation was nearing completion, a paper by Barnett and Asaro [17] appeared in which slit-like cracks in arbitrary anisotropic media are studied. However, they point out that their analysis is only analytically convenient for predicting general properties such as the crack extension forces and the energy of deformation. In contrast, the results reported here for an orthotropic crystal are shown to be ideally suited for deriving detailed formulae for the stress components and in particular for their angular variation around the crack tip for all three modes of loading.

* On leave from School of Mathematics, University of Bradford, Bradford, England.

The content of later sections of this paper is, in brief, as follows. In section 2, the problem is formulated by describing the orientation of the crack and the coordinate system with respect to the orthotropic crystal and specifying the three fundamental modes (I, II, III) of loading which are customarily applied to the crack surface. Ways of particularizing the subsequent analyses to hexagonal and cubic crystals are indicated. Sections 3, 4 and 5 are concerned with deriving and analyzing the stress fields' components for mode II, mode I and mode III cracks respectively. Closed form expressions are first obtained for these components and then appropriate approximations valid near the crack tip are derived. Representative numerical results illustrating and supplementing the analyses are presented and comparable results are given for an isotropic material. Elastoplastic cracks are discussed in section 6 using the BCS model.

2. Formulation of the problem

We consider a plane, stationary, Griffith-type strip crack of width $2c$ in a homogeneous crystal which is orthotropically symmetric in its elastic response. The material is assumed to be initially everywhere at rest and stress-free in a natural reference state and situated so that its three mutually perpendicular planes of symmetry are the coordinate planes of a system of rectangular Cartesian coordinates x, y, z.

The crack is assumed to occupy the region $-c < x < c$, $y = 0$, $-\infty < z < \infty$ of the x–z plane. We shall follow the practice, which has become customary in fracture mechanics, of distinguishing three modes of traction applied to the surfaces of the crack:

$$\begin{aligned} &\text{Mode I:} \quad \sigma_{yy}(x,0) = T(x), \quad \sigma_{xy}(x,0) = 0 \ ; \\ &\text{Mode II:} \quad \sigma_{yy}(x,0) = 0, \quad \sigma_{xy}(x,0) = T(x) \ ; \\ &\text{Mode III:} \quad \sigma_{yz}(x,0) = T(x), \end{aligned} \tag{1}$$

where $\sigma_{xy}, \sigma_{xx}, \sigma_{yy}, \sigma_{yz}$ are the components of the stress tensor referred to the coordinates x, y, z and $T(x)$ is a prescribed function. The first two modes constitute plane strain deformations and the third antiplane strain.

For an orthotropic material, the relation connecting the components of the stress and strain tensors $\boldsymbol{\sigma}$ and $\boldsymbol{\varepsilon}$, respectively, referred to the x, y, z coordinate system can be written in the form

$$\begin{pmatrix} \sigma_{11} \\ \sigma_{22} \\ \sigma_{33} \\ \sigma_{23} \\ \sigma_{13} \\ \sigma_{12} \end{pmatrix} = \begin{pmatrix} c_{11} & c_{12} & c_{13} & 0 & 0 & 0 \\ c_{12} & c_{22} & c_{23} & 0 & 0 & 0 \\ c_{13} & c_{23} & c_{33} & 0 & 0 & 0 \\ 0 & 0 & 0 & 2c_{44} & 0 & 0 \\ 0 & 0 & 0 & 0 & 2c_{55} & 0 \\ 0 & 0 & 0 & 0 & 0 & 2c_{66} \end{pmatrix} \begin{pmatrix} \varepsilon_{11} \\ \varepsilon_{22} \\ \varepsilon_{33} \\ \varepsilon_{23} \\ \varepsilon_{13} \\ \varepsilon_{12} \end{pmatrix} \tag{2}$$

where the c_{ij} denote the elastic constants referred to the chosen coordinate system.

Particularly important classes of orthotropic crystals are hexagonal and cubic crystals. It is convenient at this stage to explicitly indicate the substitutions which can be made into the expression (2) to reduce the nine elastic constants to the five or three constants, respectively, which are appropriate for a hexagonal or cubic crystal.

Consider a hexagonal crystal placed with the y-axis of our coordinate system directed along its six-fold axis of symmetry, so that the x–z plane in which the crack is situated is the basal plane. The elastic constants are known to be rotationally invariant with respect to the hexagonal axis. It is perhaps worthwhile emphasizing that the orientation of coordinate system relative to the hexagonal crystal which is appropriate for the crack analysis is that used by Chou [14] and is not the standard system (z-axis parallel to the six-fold axis) for a hexagonal lattice. All our subsequent results and analyses for the orthotropic crystal can be reduced to those for a

crack in the basal plane of the hexagonal crystal by making the substitutions

$$c_{13} = c_{12}{}^h, \quad c_{12} = c_{23} = c_{13}{}^h, \quad c_{22} = c_{33}{}^h,$$
$$c_{11} = c_{33} = c_{11}{}^h, \quad c_{55} = \tfrac{1}{2}(c_{11}{}^h - c_{12}{}^h), \quad c_{44} = c_{66} = c_{44}{}^h.$$

throughout, where the superscript h is used to indicate that the five elastic constants are those of a hexagonal crystal referred to the standard coordinate system.

For a cubic crystal situated with the x, y, z axes coinciding with its three cubic edges the substitutions which are needed throughout to make our analyses appropriate for discussing the crack in the x–z plane are

$$c_{13} = c_{23} = c_{12}{}^c, \quad c_{22} = c_{33} = c_{11}{}^c, \quad c_{55} = c_{66} = c_{44}{}^c.$$

Our results are also convenient for discussing the crack when the x and y axes are rotated relative to the cubic crystal through an angle $\pi/4$ about the z-axis. The appropriate substitutions to make can be deduced from Chou *et al.* [15, 16].

We first discuss a shear crack subjected to mode II surface tractions.

3. Inplane shear crack

According to the general procedure of the dislocation layer method, a loaded crack can be discussed by replacing it by a continuous planar distribution of dislocations. For this mode II shear crack it is appropriate to use stationary straight edge dislocations with line in the z-direction and Burgers vector in the x-direction. We assume that a dislocation of this type corresponds to a displacement discontinuity given by

$$\mathbf{u}^{\mathrm{II}}(x, 0+) - \mathbf{u}^{\mathrm{II}}(x, 0-) = (-b, 0, 0) \quad \text{for} \quad x > 0$$

where b is a constant. The superfix II is attached to the displacement $\mathbf{u}$ and the components of the stress tensor for this dislocation throughout this section. The stress field of such a dislocation situated at the origin has been derived by Chou and Sha [13] and has components given by

$$\begin{aligned}
\sigma_{xy}^{\mathrm{II}}(x, y) &= \frac{bK_e x}{2\pi} \frac{x^2 - \lambda^2 y^2}{(x^2 - \lambda^2 y^2)^2 + d^2 \lambda^2 x^2 y^2} \\
\sigma_{xx}^{\mathrm{II}}(x, y) &= -\frac{bK_e \lambda^2 y}{2\pi} \frac{\{(C+3)x^2 + \lambda^2 y^2\}}{(x^2 - \lambda^2 y^2)^2 + d^2 \lambda^2 x^2 y^2} \\
\sigma_{yy}^{\mathrm{II}}(x, y) &= \frac{bK_e y}{2\pi} \frac{x^2 - \lambda^2 y^2}{(x^2 - \lambda^2 y^2)^2 + d^2 \lambda^2 x^2 y^2}
\end{aligned} \tag{3}$$

where the constants K_e, λ^2, C and d are given in terms of the elastic constants c_{ij} by

$$\begin{aligned}
K_e &= (\bar{c}_{12} + c_{12}) \left\{ \frac{c_{66}(\bar{c}_{12} - c_{12})}{c_{22}(\bar{c}_{12} + c_{12} + 2c_{66})} \right\}^{\frac{1}{2}} \\
\lambda^2 &= (c_{11}/c_{22})^{\frac{1}{2}}, \\
C &= (\bar{c}_{12} + c_{12})(\bar{c}_{12} - c_{12} - 2c_{66})/(\bar{c}_{12} c_{66}), \\
d^2 &= C + 4 = (\bar{c}_{12} - c_{12})(\bar{c}_{12} + c_{12} + 2c_{66})/(\bar{c}_{12} c_{66}), \\
\bar{c}_{12} &= (c_{11} c_{22})^{\frac{1}{2}}.
\end{aligned} \tag{4}$$

We see from equation (3_1) that on $y = 0$, where the boundary condition (1_2) must be satisfied, $\sigma_{xy}^{\mathrm{II}}$ is given by

$$\sigma_{xy}^{\mathrm{II}}(x, 0) = \frac{bK_e}{2\pi} \frac{1}{x}. \tag{5}$$

If we suppose that the density of the proposed distribution of dislocations on $y = 0$ is $f(x)$, so that the number of dislocations in the interval $(x, x+dx)$ is $f(x)dx$ for all $|x| < c$, then,

recalling (5), the corresponding stress component at a point on the x-axis is given by

$$\sigma_{xy}(x, 0) = \int_{-c}^{c} \sigma_{xy}^{II}(x-x', 0) f(x') dx' = \frac{bK_e}{2\pi} \int_{-c}^{c} \frac{f(x')}{x-x'} dx' . \tag{6}$$

By using the Plemelj formulae and equation (3_1) to evaluate

$$\sigma_{xy}(x, 0) = \lim_{y \to 0} \int_{-c}^{c} \sigma_{xy}^{II}(x-x', 0) f(x') dx' ,$$

it is clear that the integral in (6) must be interpreted as a Cauchy principal value integral.

Setting the expression (6) equal to $T(x)$ for $|x| < c$, to satisfy the second of the boundary conditions (1_2), yields a singular integral equation for the density function $f(x)$ whose general solution is well-known [18, 19]. We impose the additional restriction that there is no relative displacement of the two crack faces at $x = \pm c$ and the appropriate solution for $f(x)$ is then found to be

$$f(x) = \frac{2}{\pi b K_e} \frac{1}{(c^2-x^2)^{\frac{1}{2}}} \int_{-c}^{c} \frac{(c^2-x'^2)^{\frac{1}{2}}}{x'-x} T(x') dx' . \tag{7}$$

This expression can now be substituted directly into the formula

$$\sigma_{ij}(x, y) = \int_{-c}^{c} \sigma_{ij}^{II}(x-x'', y) f(x'') dx'' \tag{8}$$

to calculate any of the stress components created by the crack. Equations (3) give the appropriate expressions for σ_{ij}^{II} and so the resulting integrals clearly all have integrands whose denominators involve the factor

$$D = \{(x-x'')^2 - \lambda^2 y^2\}^2 + d^2 \lambda^2 (x-x'')^2 y^2 . \tag{9}$$

This quartic expression can be factorized into the product of quadratic factors in two different ways which yield

$$D = \{(x-x'')^2 + [d+(d^2-4)^{\frac{1}{2}}]^2 (\lambda y/2)^2\} \{(x-x'')^2 + [d-(d^2-4)^{\frac{1}{2}}]^2 (\lambda y/2)^2\} \tag{10}$$

and

$$D = [\{x-x''+(4-d^2)^{\frac{1}{2}}(\lambda y/2)\}^2 + (d\lambda y/2)^2][\{x-x''-(4-d^2)^{\frac{1}{2}}(\lambda y/2)\}^2 + (d\lambda y/2)^2] . \tag{11}$$

Recalling from equation (4_4) that $C = d^2 - 4$, the factorization (10) is found to be appropriate if $C > 0$ whilst (11) is useful when $C < 0$. The value of C depends upon the elastic constants of the medium, but Chou and Sha [13] and Chou [14] have stated that the inequality $C > -4$ always holds. For convenience and brevity, however, we restrict our discussion in this and the following section to materials for which $C > 0$. The corresponding results for $C < 0$ can be derived similarly by straight-forward, but tedious, manipulations using the factorization (11). As an illustration, the stress components for the mode II crack are given in Appendix I.

For $d^2 - 4 > 0$, the integrals for the σ_{ij} can be simplified by splitting them into partial fractions using the factorization (10) and then making use of the two integrals whose values are stated in Appendix II with $\mathscr{K} = [d \pm (d^2-4)^{\frac{1}{2}}](\lambda/2)$. These manipulations yield

$$\begin{aligned}
\sigma_{xy}(x, y) &= \tfrac{1}{2}\{[d+(d^2-4)^{\frac{1}{2}}]\mathscr{F}_+(\theta_+) - [d-(d^2-4)^{\frac{1}{2}}]\mathscr{F}_-(\theta_-)\} , \\
\sigma_{xx}(x, y) &= -\lambda \left\{ \frac{d(d^2-3)+(d^2-1)(d^2-4)^{\frac{1}{2}}}{d+(d^2-4)^{\frac{1}{2}}} \mathscr{F}_+(\theta_+ - \pi/2) \right. \\
&\qquad \left. - \frac{d(d^2-3)-(d^2-1)(d^2-4)^{\frac{1}{2}}}{d-(d^2-4)^{\frac{1}{2}}} \mathscr{F}_-(\theta_- - \pi/2) \right\} \\
\sigma_{yy}(x, y) &= \frac{1}{\lambda} \{\mathscr{F}_+(\theta_+ - \pi/2) - \mathscr{F}_-(\theta_- - \pi/2)\} .
\end{aligned} \tag{12}$$

where the functions $\mathscr{F}_+(\theta_+)$ and $\mathscr{F}_-(\theta_-)$, which arise in section 4 also, are defined by

$$\mathscr{F}_{\pm}(\theta_{\pm}) =$$

$$= \frac{1}{\pi(d^2-4)^{\frac{1}{2}}} \int_{-c}^{c} \frac{\{[d\pm(d^2-4)^{\frac{1}{2}}](\lambda y/2)\cos\theta_{\pm} + (x-x')\sin\theta_{\pm}\}}{R_{\pm}\{(x-x')^2 + [d\pm(d^2-4)^{\frac{1}{2}}]^2(\lambda y/2)^2\}} (c^2-x'^2)^{\frac{1}{2}} T(x')dx' . \quad (13)$$

The quantities $R_+(x, y)$, $R_-(x, y)$, $\theta_+(x, y)$ and $\theta_-(x, y)$ are given by

$$R_{\pm}\, e^{i\theta_{\pm}} = [c^2 - \{x + i[d\pm(d^2-4)^{\frac{1}{2}}](\lambda y/2)\}^2]^{\frac{1}{2}} . \quad (14)$$

A cut is introduced in the x, y-plane extending along the x-axis between the branch points $x = \pm c$. Branches of the square root function are determined by choosing $\theta_{\pm}$ to be zero for $|x| < c$, $y = 0+$ and defining it by analytic continuation elsewhere. The Plemelj formulae immediately show from equation (12_3) that $\lim_{y\to 0} \sigma_{yy}(x, y) = 0$ and hence the first of the two boundary conditions (1_2) on the crack is indeed satisfied.

The important features of crack-tip stress distributions can be demonstrated by setting

$$x = c + r\cos\alpha , \quad y = r\sin\alpha$$

where $r \ll c$. From equation (14), the corresponding approximations to $R_{\pm}$ and $\theta_{\pm}$ are found to be

$$R_{\pm} \sim [2cr\{\cos^2\alpha + (d\pm(d^2-4)^{\frac{1}{2}})^2(\lambda/2)^2\sin^2\alpha\}^{\frac{1}{2}}]^{\frac{1}{2}} , \quad \theta_{\pm} \sim -(\pi-\phi_{\pm})/2 \quad (15)$$

as $r\to 0$, where

$$\phi_{\pm} = \tan^{-1}\{[d\pm(d^2-4)^{\frac{1}{2}}](\lambda/2)\tan\alpha\} \quad (16)$$

with $\tan^{-1}(\ldots)$ being understood to indicate the principal value of the inverse tangent for $0 \leqq \alpha < \pi/2$ and π plus the principal value for $\pi/2 \leqq \alpha \leqq \pi$. Substituting these into equations (12) and (13) and putting

$$\Delta_{\pm} = \{\cos^2\alpha + [d\pm(d^2-4)^{\frac{1}{2}}]^2(\lambda/2)^2\sin^2\alpha\}^{\frac{1}{4}} , \quad (17)$$

we obtain

$$\sigma_{xy}(r, \alpha) \sim \frac{1}{2(d^2-4)^{\frac{1}{2}}} \left\{ \frac{d+(d^2-4)^{\frac{1}{2}}}{\Delta_+}\cos(\phi_+/2) - \frac{d-(d^2-4)^{\frac{1}{2}}}{\Delta_-}\cos(\phi_-/2) \right\} \frac{K}{r^{\frac{1}{2}}} ,$$

$$\sigma_{xx}(r, \alpha) \sim -\frac{\lambda}{(d^2-4)^{\frac{1}{2}}} \left\{ \frac{d(d^2-3)+(d^2-1)(d^2-4)^{\frac{1}{2}}}{[d+(d^2-4)^{\frac{1}{2}}]\Delta_+}\sin(\phi_+/2) \right.$$

$$\left. - \frac{d(d^2-3)+(d^2-1)(d^2-4)^{\frac{1}{2}}}{[d-(d^2-4)^{\frac{1}{2}}]\Delta_-}\sin(\phi_-/2) \right\} \frac{K}{r^{\frac{1}{2}}} ,$$

$$\sigma_{yy}(r, \alpha) \sim \frac{1}{\lambda(d^2-4)^{\frac{1}{4}}} \left\{ \frac{\sin(\phi_+/2)}{\Delta_+} - \frac{\sin(\phi_-/2)}{\Delta_-} \right\} \frac{K}{r^{\frac{1}{2}}} . \quad (18)$$

as $r\to 0$, with

$$K = -\frac{1}{\pi(2c)^{\frac{1}{2}}} \int_{-c}^{c} \left(\frac{c+x'}{c-x'}\right)^{\frac{1}{2}} T(x')dx' . \quad (19)$$

The radial shear stress component, $\sigma_{r\alpha}$, is perhaps the most physically important and it follows from equations (18) that this is given by

$$\sigma_{r\alpha}(r, \alpha) \sim \frac{1}{2(d^2-4)^{\frac{1}{2}}} \left[\left\{ \left(\frac{1}{\lambda} + \frac{\lambda\{d(d^2-3)+(d^2-1)(d^2-4)^{\frac{1}{2}}\}}{d+(d^2-4)^{\frac{1}{2}}} \right) \frac{\sin(\phi_+/2)}{\Delta_+} \right.\right.$$

$$\left. - \left(\frac{1}{\lambda} + \frac{\lambda\{d(d^2-3)-(d^2-1)(d^2-4)^{\frac{1}{2}}\}}{d-(d^2-4)^{\frac{1}{2}}} \right) \frac{\sin(\phi_-/2)}{\Delta_-} \right\} \sin 2\alpha$$

$$\left. + \left\{ [d+(d^2-4)^{\frac{1}{2}}] \frac{\cos(\phi_+/2)}{\Delta_+} - [d-(d^2-4)^{\frac{1}{2}}] \frac{\cos(\phi_-/2)}{\Delta_-} \right\} \cos 2\alpha \right] \frac{K}{r^{\frac{1}{2}}} \quad (20)$$

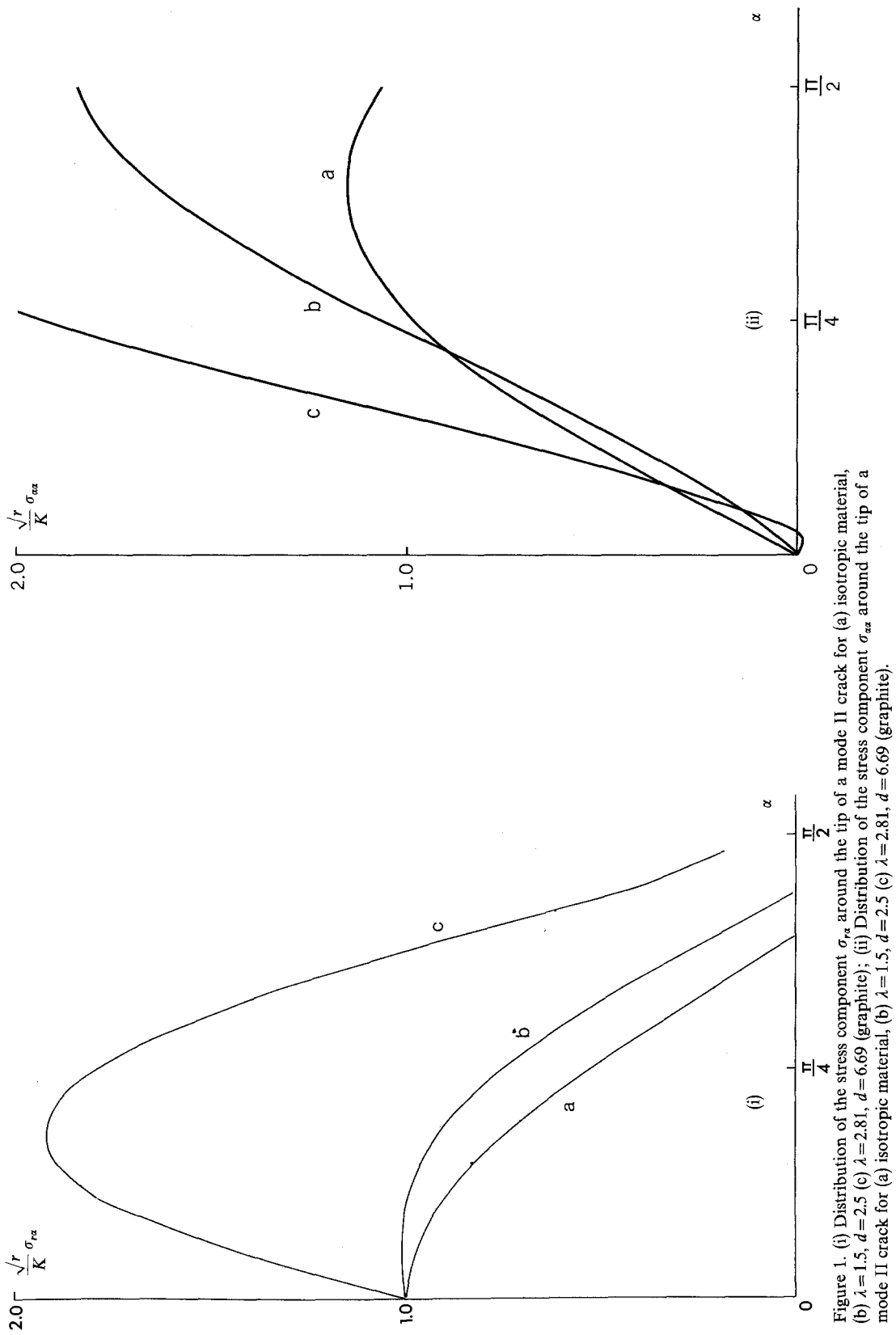

Figure 1. (i) Distribution of the stress component σ_{rr} around the tip of a mode II crack for (a) isotropic material, (b) $\lambda = 1.5$, $d = 2.5$ (c) $\lambda = 2.81$, $d = 6.69$ (graphite); (ii) Distribution of the stress component $\sigma_{\alpha\alpha}$ around the tip of a mode II crack for (a) isotropic material, (b) $\lambda = 1.5$, $d = 2.5$ (c) $\lambda = 2.81$, $d = 6.69$ (graphite).

as $r \to 0$.

It is interesting to observe at this stage that the stress components near the end $x=c$ of this mode II crack are dependent upon the surface traction $T(x)$ only through the factor K defined by equation (19). The subsequent analyses of sections 4 and 5 show that the same observation can be made for either a mode I or mode III crack. K, in fact, is simply the corresponding stress intensity factor at the tip $x=c$ of a stationary or moving crack in an isotropic material. We note that on the x-axis ahead of the crack ($\alpha=0$) the stress components have the behaviour

$$\sigma_{xy}(r, 0) \sim K/r^{\frac{1}{2}}, \quad \sigma_{yy}(r, 0) \sim 0$$

as $r \to 0$, which is clearly independent of the anisotropy of the properties of the medium.

The approximate variation of $\sigma_{r\alpha}$ with the angle α for a fixed value of r for any orthotropically symmetric crystal for which $C>0$ can be investigated by substituting the appropriate values of λ and d into the expression (20). Recalling the substitutions mentioned at the end of section 2, the values of λ and d for various hexagonal and cubic crystals have been calculated using the data of Huntingdon [20] and Chou [14]. In fact it is found that for many of these λ and d have values which are close to those of an isotropic material ($\lambda=1$, $d=2$) and the results are correspondingly similar. However, for graphite ($\lambda=2.81$, $d=6.69$), for example, the results have the significantly different property of the maximum stress occurring in a non-forward direction (i.e. off the x-axis). This property occurs for any crystals with values of λ and d large compared to those of an isotropic material. Typically, Figure 1(i) illustrates the distribution of the scaled stress component, $r^{\frac{1}{2}}\sigma_{r\alpha}/K$, around the tip $x=c$, of a crack in graphite and for the case $\lambda=1.5$, $d=2.5$. For comparison, the corresponding curve for an isotropic material is also depicted. (This curve is graphically indistinguishable from that of cobalt ($\lambda=0.96, d=2.32$) and magnesium ($\lambda=0.992$, $d=2.124$), for example).

The approximate expression for $\sigma_{r\alpha}$ for an isotropic medium does not appear to have been presented explicitly elsewhere. It can be deduced by taking the limit as $d \to 2$ and $\lambda \to 1$ in the approximation (20) but alternatively, and perhaps more conveniently, the results of Lardner [6, section 5.2] also yield

$$\sigma_{r\alpha} \sim \left(\tfrac{1}{2} \sin\alpha \sin\frac{\alpha}{2} + \cos\frac{3\alpha}{2}\right)\frac{K}{r^{\frac{1}{2}}}$$

as $r \to 0$, for an isotropic material. The main conclusion which can be drawn therefore is that, in contrast to the isotropic case, the stress component $\sigma_{r\alpha}$ in a strongly anisotropically orthotropic crystal has a maximum in a non-forward direction.

We can also calculate the tangential stress component $\sigma_{\alpha\alpha}=\sigma_{xx}\sin^2\alpha+\sigma_{yy}\cos^2\alpha-\sigma_{xy}\sin 2\alpha$ in the neighbourhood of the crack tip using the asymptotic forms of the stresses in equations (18). The angular variation of $r^{\frac{1}{2}}\sigma_{\alpha\alpha}/K$ around the tip $x=c$ is illustrated in Figure 1(ii) for a range of values of λ and d. The curve (a) exhibits the well-known property that in an isotropic material $\sigma_{\alpha\alpha}$ has a maximum at about $-70°$. It is often concluded that a crack in a brittle material subject to shear forces will grow in a tensile mode at an angle of $-70°$ to its initial direction. As the strength of anisotropy increases, it is found that the maximum in $\sigma_{\alpha\alpha}$ becomes sharper and also moves round towards an angle of $-90°$ with the crack.

Similiar properties to the above were found and discussed for the corresponding components $\sigma_{r\alpha}$ and $\sigma_{\alpha\alpha}$ in the situation studied by Lardner and Tupholme [9].

4. Normally loaded crack

The analysis of this section is presented rather more briefly than that of section 3 as the underlying techniques are very similar. The mode I crack discussed here can again be represented by a distribution of edge dislocations. To satisfy the boundary conditions (1_1) it is clearly necessary to make use of dislocations whose Burgers vectors are in the y-direction.

If we assume that the appropriate displacement discontinuity across the plane $y=0$ is given by

$$\mathbf{u}^{\mathrm{I}}(x, 0+)-\mathbf{u}^{\mathrm{I}}(x, 0-)=(0, b, 0) \quad \text{for} \quad x>0,$$

the corresponding stress field of such a dislocation situated at the origin has components (see [13]) given by

$$\left.\begin{aligned}
\sigma_{xy}^{\mathrm{I}}(x, y) &= -\frac{bK_n\lambda^2 y}{2\pi}\frac{x^2-\lambda^2y^2}{(x^2-\lambda^2y^2)^2+d^2\lambda^2x^2y^2},\\
\sigma_{xx}^{\mathrm{I}}(x, y) &= -\frac{bK_n\lambda^2 x}{2\pi}\frac{x^2-\lambda^2y^2}{(x^2-\lambda^2y^2)^2+d^2\lambda^2x^2y^2},\\
\sigma_{yy}^{\mathrm{I}}(x, y) &= -\frac{bK_n x}{2\pi}\frac{x^2+(C+3)\lambda^2y^2}{(x^2-\lambda^2y^2)+d^2\lambda^2x^2y^2}
\end{aligned}\right\} \tag{21}$$

where

$$K_n = K_e(c_{22}/c_{11})^{\frac{1}{2}}. \tag{22}$$

From equation (21_3) we see that $\sigma_{yy}^{\mathrm{I}}(x, 0)$ is given by the right-hand side of equation (5) with K_e replaced by $-K_n$ and equation (7) therefore shows that the mode I crack can be replaced by a distribution of climb edge dislocations with density function $f(x)$ given by

$$f(x) = -\frac{2}{\pi bK_n}\frac{1}{(c^2-x^2)^{\frac{1}{2}}}\int_{-c}^{c}\frac{(c^2-x'^2)^{\frac{1}{2}}}{x'-x}T(x')dx'.$$

As is the previous section, the corresponding expressions for the stress components of the mode I crack, which can be calculated from the formula

$$\sigma_{ij}(x, y) = \int_{-c}^{c}\sigma_{ij}^{\mathrm{I}}(x-x'', y)f(x'')dx'',$$

depend upon whether the constant C is positive or negative. Restricting our attention to cases for which $C>0$, we find using the results (A.3) and (A.4) that

$$\left.\begin{aligned}
\sigma_{xy}(x, y) &= \lambda\{\mathscr{F}_+(\theta_+-\pi/2)-\mathscr{F}_-(\theta_--\pi/2)\},\\
\sigma_{xx}(x, y) &= \frac{\lambda^2}{2}\{[d+(d^2-4)^{\frac{1}{2}}]\mathscr{F}_+(\theta_+)-[d-(d^2-4)^{\frac{1}{2}}]\mathscr{F}_-(\theta_-)\},\\
\sigma_{yy}(x, y) &= -\tfrac{1}{2}\{[d-(d^2-4)^{\frac{1}{2}}]\mathscr{F}_+(\theta_+)-[d+(d^2-4)^{\frac{1}{2}}]\mathscr{F}_-(\theta_-)\},
\end{aligned}\right\} \tag{23}$$

where $\mathscr{F}_\pm(\theta_\pm)$, $R_\pm$ and $\theta_\pm$ are given by equations (13) and (14). This solution does indeed solve the problem for the mode I crack since the second of the boundary conditions (1_1) is satisfied by the expression (23_1) for σ_{xy}.

Using the approximations (15) and (16) near the crack tip and the definitions (17) and (19) of $\Delta_\pm$ and K, respectively, it follows that

$$\left.\begin{aligned}
\sigma_{xy}(r, \alpha) &\sim \frac{\lambda}{(d^2-4)^{\frac{1}{2}}}\left\{\frac{\sin(\phi_+/2)}{\Delta_+}-\frac{\sin(\phi_-/2)}{\Delta_-}\right\}\frac{K}{r^{\frac{1}{2}}},\\
\sigma_{xx}(r, \alpha) &\sim \frac{\lambda^2}{2(d^2-4)^{\frac{1}{2}}}\left\{\frac{d+(d^2-4)^{\frac{1}{2}}}{\Delta_+}\cos(\phi_+/2)-\frac{d-(d^2-4)^{\frac{1}{2}}}{\Delta_-}\cos(\phi_-/2)\right\}\frac{K}{r^{\frac{1}{2}}}\\
\sigma_{yy}(r, \alpha) &\sim -\frac{1}{2(d^2-4)^{\frac{1}{2}}}\left\{\frac{d-(d^2-4)^{\frac{1}{2}}}{\Delta_+}\cos(\phi_+/2)-\frac{d+(d^2-4)^{\frac{1}{2}}}{\Delta_-}\cos(\phi_-/2)\right\}\frac{K}{r^{\frac{1}{2}}}
\end{aligned}\right\} \tag{24}$$

as $r\to 0$. The corresponding tangential stress component $\sigma_{\alpha\alpha}$ can easily be calculated from the formula $\sigma_{\alpha\alpha}=\sigma_{xx}\sin^2\alpha+\sigma_{yy}\cos^2\alpha-\sigma_{xy}\sin 2\alpha$ and it is found to exhibit the same principle factors as $\sigma_{r\alpha}$ in the shear case. In particular, a non-forward maximum develops as λ and d increase. Again, as $r\to 0$ the components $\sigma_{xy}(r, 0)$ and $\sigma_{yy}(r, 0)$ do not depend upon the elastic

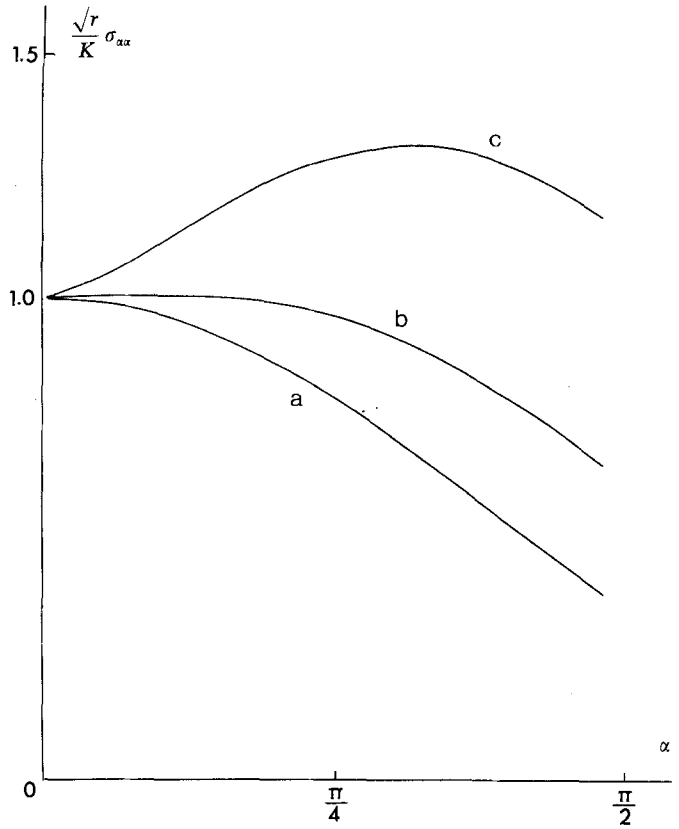

Figure 2. Distribution of the stress component $\sigma_{\alpha\alpha}$ around the tip of a mode I crack for (a) isotropic material, (b) $\lambda = 1.5$, $d = 2.5$, (c) $\lambda = 2.81$, $d = 6.69$ (graphite).

constants of the material. Figure 2 illustrates the variation of the scaled stress component, $r^{\frac{1}{2}}\sigma_{\alpha\alpha}/K$, around the crack tip for graphite ($\lambda = 2.81$, $d = 6.69$) and the case $\lambda = 1.5$, $d = 2.5$. For an isotropic material

$$\sigma_{\alpha\alpha} \sim \left(\cos\frac{\alpha}{2} - \frac{1}{2}\sin\alpha\,\sin\frac{\alpha}{2}\right)\frac{K}{r^{\frac{1}{2}}}$$

as $r \to 0$ and the curve representing this is also shown.

5. Antiplane shear crack

A mode III crack can be replaced by a distribution of screw dislocations with density function $f(x)$ whose displacement discontinuities are given by

$$\mathbf{u}^{\mathrm{III}}(x, 0+) - \mathbf{u}^{\mathrm{III}}(x, 0-) = (0, 0, -b) \quad \text{for} \quad x > 0\,.$$

For a screw dislocation of this type situated at the origin, the stress field has non-zero components [13] given by

$$\left.\begin{aligned} \sigma_{xz}^{\mathrm{III}}(x, y) &= -\frac{bK_s}{2\pi}\frac{\eta^2 y}{x^2 + \eta^2 y^2}, \\ \sigma_{yz}^{\mathrm{III}}(x, y) &= \frac{bK_s}{2\pi}\frac{x}{x^2 + \eta^2 y^2} \end{aligned}\right\} \tag{25}$$

where

$$K_s = (c_{44}c_{55})^{\frac{1}{2}}, \quad \eta^2 = (c_{55}/c_{44})^{\frac{1}{2}}\,. \tag{26}$$

By comparing the right-hand side of equation (5) with

$$\sigma_{yz}^{\mathrm{III}}(x, 0) = \frac{bK_s}{2\pi}\frac{1}{x},$$

the analysis (with K_e replaced by K_s) leading to equation (7) is seen to be applicable to show that

$$f(x) = \frac{2}{\pi b K_s}\frac{1}{(c^2-x^2)^{\frac{1}{2}}}\int_{-c}^{c}\frac{(c^2-x'^2)^{\frac{1}{2}}}{x'-x}T(x')dx'.$$

Define quantities $\mathscr{E}(\theta)$, $R(x, y)$ and $\theta(x, y)$ by

$$\left.\begin{aligned}\mathscr{E}(\theta) &= \frac{1}{\pi}\int_{-c}^{c}\frac{\eta y\cos\theta+(x-x')\sin\theta}{R\{(x-x')^2+\eta^2y^2\}}(c^2-x'^2)^{\frac{1}{2}}T(x')dx',\\ R\,\mathrm{e}^{\mathrm{i}\theta} &= \{c^2-(x+\mathrm{i}\eta y)^2\}^{\frac{1}{2}}\end{aligned}\right\} \tag{27}$$

with θ chosen to be zero on $y=0+$ for $|x|<c$ and continued analytically elsewhere. It then follows, from the formula

$$\sigma_{ij}(x, y) = \int_{-c}^{c}\sigma_{ij}^{\mathrm{III}}(x-x'', y)f(x'')dx'',$$

that for all η

$$\left.\begin{aligned}\sigma_{xz}(x, y) &= -\eta\mathscr{E}(\theta-\pi/2),\\ \sigma_{yz}(x, y) &= \mathscr{E}(\theta).\end{aligned}\right\} \tag{28}$$

From these expressions, we find that near the crack tip

$$\left.\begin{aligned}\sigma_{xz}(r, \alpha) &\sim -\eta\frac{\sin(\phi/2)}{\Delta}\frac{K}{r^{\frac{1}{2}}},\\ \sigma_{yz}(r, \alpha) &\sim \frac{\cos(\phi/2)}{\Delta}\frac{K}{r^{\frac{1}{2}}}\end{aligned}\right\} \tag{29}$$

as $r\to 0$, where K is defined by equation (19) and

$$\left.\begin{aligned}\Delta &= (\cos^2\alpha+\eta^2\sin^2\alpha)^{\frac{1}{4}}\\ \phi &= \tan^{-1}(\eta\tan\alpha).\end{aligned}\right\} \tag{30}$$

Clearly, the anisotropy of the material again does not affect $\sigma_{xz}(r, 0)$ or $\sigma_{yz}(r, 0)$ near the crack tip.

Equations (29) yield an expression for the stress component $\sigma_{\alpha z}$ near the crack tip of the form

$$\sigma_{\alpha z}(r, \alpha) \sim \left\{\frac{\eta\sin(\phi/2)\sin\alpha+\cos(\phi/2)\cos\alpha}{\Delta}\right\}\frac{K}{r^{\frac{1}{2}}} \tag{31}$$

as $r\to 0$. The component $\sigma_{\alpha z}$ develops a non-forward maximum as the value of η increases. The critical value at which this first occurs is $\eta\approx 1.41$. Figure 3 shows graphically the variation with α of the scaled stress component $r^{\frac{1}{2}}\sigma_{\alpha z}/K$ around the crack tip $x=c$ for graphite ($\eta=1.36$) using the data [14, 20]. For an isotropic material it is found, by letting $\eta\to 1$ in equation (31), that

$$\sigma_{\alpha z} \sim \cos\left(\frac{\alpha}{2}\right)\frac{K}{r^{\frac{1}{2}}}$$

as $r\to 0$. The curves representing this and the cases $\eta=2.5$, $\eta=4$ are also included in Figure 3 for comparison.

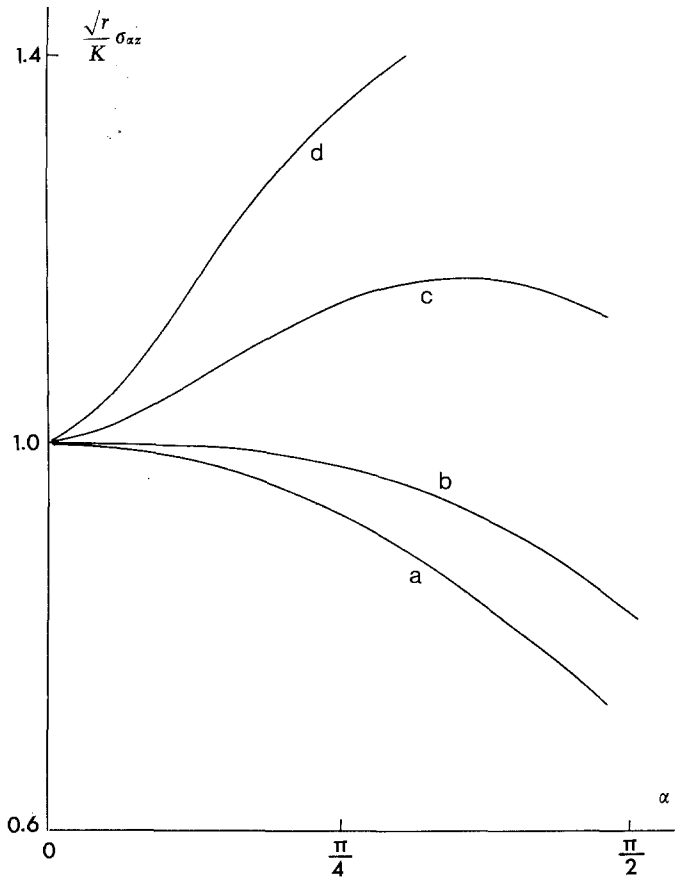

Figure 3. Distribution on the stress component σ_{xz} around the tip of a mode III crack for (a) isotropic material, (b) $\eta=1.36$ (graphite), (c) $\eta=2.5$, (d) $\eta=4.0$.

6. Elastoplastic crack

The BCS model [21] proposes that the plastic zones of a mode II crack with plastic flow at its tips can be considered as a planar distribution of dislocations extending over the regions $c<|x|<a$. (These plastic zones are symmetrical about $x=0$ provided we assume that the surface traction $T(x)$ is an even function of x for $|x|<c$.) Suppose that within these regions $\sigma_{xy}(x, 0)=-\sigma_1$, the constant yield stress of the material.

Since $\sigma_{xy}(x, 0)$ is required to have no singularities at the tips $x=\pm a$ of the two plastic zones, the stress intensity factor there, obtainable by comparison with equation (19), must vanish. It follows that

$$\sigma_1 \int_{c<|x'|<a} \frac{dx'}{(a^2-x'^2)^{\frac{1}{2}}} = \int_{-c}^{c} \frac{T(x')dx'}{(a^2-x'^2)^{\frac{1}{2}}}.$$

This result determines the length $(a-c)$ of the plastic regions and is identical to that corresponding to an isotropic material. From equation (7), the density of dislocations in the region $|x|<a$ can be deduced to be

$$f(x) = \frac{2}{\pi b K_e} \frac{1}{(a^2-x^2)^{\frac{1}{2}}} \left\{ \int_{-c}^{c} \frac{(a^2-x'^2)^{\frac{1}{2}}}{x'-x} T(x')dx' - \sigma_1 \int_{c<|x'|<a} \frac{(a^2-x'^2)^{\frac{1}{2}}}{x'-x} dx' \right\},$$

which is simply that of the isotropic case multiplied by a factor $\mu/K_e(1-\nu)$, μ and ν being the shear modulus and Poisson's ratio, respectively, of the isotropic solid in its reference state. The ratio Φ_0^{II}/Φ_i^{II} of the plastic displacement at the tip of the crack $(\int_c^a bf(x)dx)$ in the orthotropic

crystal to that in an isotropic material is therefore given by

$$\Phi_0^{\mathrm{II}}/\Phi_{\mathrm{i}}^{\mathrm{II}} = \mu/K_e(1-\nu)\,.$$

If the same model is applied to mode I and III elastoplastic cracks, it is found that, in a self-explanatory notation,

$$\Phi_0^{\mathrm{I}}/\Phi_{\mathrm{i}}^{\mathrm{I}} = \mu/K_n(1-\nu)\,,$$
$$\Phi_0^{\mathrm{III}}/\Phi_{\mathrm{i}}^{\mathrm{III}} = \mu/K_s$$

and the lengths of the plastic zones are again unaffected.

Appendix I

For the inplane shear crack (see section 3) in orthotropic crystals for which $d^2-4<0$, the components of the stress field are found to be as follows:

$$\left.\begin{aligned}
\sigma_{xy}(x,y) &= -\tfrac{1}{2}\{\mathscr{G}_+^{(1)}(\theta_+)-\mathscr{G}_-^{(1)}(\theta_-)\}\,,\\
\sigma_{xx}(x,y) &= \frac{\lambda}{2}\{\mathscr{G}_+^{(2)}(\theta_+)-\mathscr{G}_-^{(2)}(\theta_-)\}\,,\\
\sigma_{yy}(x,y) &= -\frac{1}{\lambda}\{\mathscr{G}_+^{(3)}(\theta_+)-\mathscr{G}_-^{(3)}(\theta_-)\}
\end{aligned}\right\} \tag{A.1}$$

where the functions $\mathscr{G}_+^{(p)}(\theta_+)$ and $\mathscr{G}_-^{(p)}(\theta_-)$ for $p=1, 2, 3$ are given by

$$\mathscr{G}_\pm^{(1)}(\theta_\pm) = \frac{1}{\pi(4-d^2)^{\frac{1}{2}}}\int_{-c}^{c} \frac{\{x-x'\pm(4-d^2)^{\frac{1}{2}}(\lambda y/2)\}\{d\cos\theta_\pm \mp(4-d^2)^{\frac{1}{2}}\sin\theta_\pm\}-\{d\sin\theta_\pm\pm(4-d^2)^{\frac{1}{2}}\cos\theta_\pm\}(\lambda dy/2)}{R_\pm\{[x-x'\pm(\lambda y/2)(4-d^2)^{\frac{1}{2}}]^2+(\lambda dy/2)^2\}}(c^2-x'^2)^{\frac{1}{2}}T(x')dx'\,,$$

$$\mathscr{G}_\pm^{(2)}(\theta_\pm) = \frac{1}{\pi(4-d^2)^{\frac{1}{2}}}\int_{-c}^{c} \frac{\{x-x'\pm(4-d^2)^{\frac{1}{2}}(\lambda y/2)\}\{\pm d(4-d^2)^{\frac{1}{2}}\cos\theta_\pm+(d^2-2)\sin\theta_\pm\}-\{\pm d(4-d^2)^{\frac{1}{2}}\sin\theta_\pm-(d^2-2)\cos\theta_\pm\}(\lambda dy/2)}{R_\pm\{[x-x'\pm(\lambda y/2)(4-d^2)^{\frac{1}{2}}]^2+(\lambda dy/2)^2\}}(c^2-x'^2)^{\frac{1}{2}}T(x')dx'\,,$$

$$\mathscr{G}_\pm^{(3)}(\theta_\pm) = \frac{1}{\pi(4-d^2)^{\frac{1}{2}}}\int_{-c}^{c} \frac{\{x-x'\pm(4-d^2)^{\frac{1}{2}}(\lambda y/2)\}\sin\theta_\pm+(\lambda dy/2)\cos\theta_\pm}{R_\pm\{[x-x'\pm(\lambda y/2)(4-d^2)^{\frac{1}{2}}]^2+(\lambda dy/2)^2\}}(c^2-x'^2)^{\frac{1}{2}}T(x')dx' \tag{A.2}$$

with

$$R_\pm\,\mathrm{e}^{\mathrm{i}\theta_+} = [c^2-\{x\pm(4-d^2)^{\frac{1}{2}}(\lambda y/2)+i\lambda dy/2\}^2]^{\frac{1}{2}}\,.$$

If required, the approximations for the stress components near the crack tip can be calculated by a technique corresponding to that used in section 3.

Appendix II

Using contour integration it can be shown that

$$\int_{-c}^{c}\frac{dx''}{(c^2-x''^2)^{\frac{1}{2}}(x'-x'')\{(x-x'')^2+\mathscr{K}^2y^2\}} = \frac{\pi\{\mathscr{K}y\sin\Theta-(x-x')\cos\Theta\}}{y\mathscr{K}\mathscr{R}\{(x-x')^2+\mathscr{K}^2y^2\}}\,, \tag{A.3}$$

$$\int_{-c}^{c}\frac{(x-x'')dx''}{(c^2-x''^2)^{\frac{1}{2}}(x'-x'')\{(x-x'')^2+\mathscr{K}^2y^2\}} = \frac{\pi\{\mathscr{K}y\cos\Theta+(x-x')\sin\Theta\}}{\mathscr{R}\{(x-x')^2+\mathscr{K}^2y^2\}} \tag{A.4}$$

for constant $\mathscr{K}$, where

$$\mathscr{R}\,\mathrm{e}^{\mathrm{i}\Theta} = \{c^2-(x+i\mathscr{K}y)^2\}^{\frac{1}{2}}$$

with the branches chosen in the same way as those of $R_\pm\,\mathrm{e}^{\mathrm{i}\theta_\pm}$ in section 3.

Acknowledgements

The author would like to take this opportunity to thank Professor R. W. Lardner for his

instructive comments throughout the course of this work and Professor Y. T. Chou for confirming several misprints in equations (6) of [14].

The results reported here were obtained during investigations supported by the Defence Research Board (Grant No. 7501-09) and the National Research Council (Grant No. A5174) of Canada.

REFERENCES

[1] I. N. Sneddon and M. Lowengrub, *Crack problems in the classical theory of elasticity*, Wiley (1969).
[2] J. R. Rice, *Fracture* (ed. H. Liebowitz), Academic Press, New York, 2 (1968) 191.
[3] C. Zener, *Fracturing of metals*, Cleveland Symposium, A.S.M., (1948).
[4] J. Friedel, *Dislocations*, Pergamon, Oxford, (1964).
[5] B. A. Bilby and J. D. Eshelby, *Fracture* (ed. H. Liebowitz), Academic Press, New York, 1 (1968) 99.
[6] R. W. Lardner, *Mathematical theory of dislocations and fracture*, University of Toronto Press, to be published.
[7] R. W. Lardner, Dislocation layers and boundary-value problems of plane elasticity, *Quart. J. Mech. Appl. Math.*, 25 (1972) 45–61.
[8] J. Guidera, *Planar distributions of dislocations*, M.Sc. thesis, Simon Fraser University (1972).
[9] R. W. Lardner and G. E. Tupholme, *Dislocation layers applied to moving crack problems*, to be published in *Int. J. Frac.*
[10] J. D. Eshelby, Edge dislocations in anisotropic materials, *Phil. Mag.*, 40 (1949) 903–912.
[11] J. D. Eshelby, W. T. Read and W. Shockley, Anisotropic elasticity with applications to dislocation theory, *Acta Met.*, 1 (1953) 251–259.
[12] A. N. Stroh, Dislocations and cracks in anisotropic elasticity, *Phil. Mag.*, 3 (1958) 625–646.
[13] Y. T. Chou and G. T. Sha, On the elastic field of a dislocation in an anisotropic crystal, *Scrip. Metal*, 5 (1971) 551–558.
[14] Y. T. Chou, Interaction of parallel dislocations in a hexagonal crystal, *J. Appl. Phys.*, 33 (1962) 2747–2751.
[15] Y. T. Chou, F. Garofalo and R. W. Whitmore, Interactions between glide dislocations in a double pile-up in α-iron, *Acta Met.*, 9 (1960) 480–488.
[16] Y. T. Chou and R. W. Whitmore, Single and double pile-up of dislocations in MgO crystals, *J. Appl. Phys.*, 32 (1961) 1920–1926.
[17] D. M. Barnett and R. J. Asaro, The fracture mechanics of slit-like cracks in anisotropic elastic media, *J. Mech. Phys. Solids*, 20 (1972) 353–366.
[18] F. D. Gakhov, *Boundary value problems*, Pergamon, Oxford (1966).
[19] N. I. Muskhelishvili, *Singular integral equations*, Noordhoff (1953).
[20] H. B. Huntingdon, *Solid State Physics* (ed. F. Seitz and D. Turnbull), Academic Press, New York, 7 (1958) 213.
[21] B. A. Bilby, A. H. Cottrell and K. Swinden, The spread of plastic yield from a notch, *Proc. Roy. Soc. A*, 272 (1963) 304–314.